Ion Heating in the Field-Reversed Configuration by Rotating Magnetic Fields near the Ion-Cyclotron Resonance

Samuel A. Cohen
Princeton University, Plasma Physics Laboratory, Princeton, New Jersey 08543

Alan H. Glasser
Los Alamos National Laboratory, P.O. Box 1663, Los Alamos, New Mexico 87545
(Received 13 July 2000)

The trajectories of ions confined in a field-reversed configuration (FRC) equilibrium magnetic geometry and heated with a small-amplitude, odd-parity rotating magnetic field (RMF) have been studied with a Hamiltonian computer code. When the RMF frequency is in the ion-cyclotron range, explosive heating occurs. Higher-energy ions are found to have betatron-type orbits, preferentially localized near the FRC's midplane. These results are relevant to a compact magnetic-fusion-reactor design.

PACS numbers: 52.50.Gj, 52.55.–s, 52.65.Cc

As a fusion reactor, the field-reversed configuration (FRC) [1] plasma-confinement device has attractive features, notably a linear magnet geometry and high-β operation ($\beta \equiv$ plasma pressure/magnetic-field pressure). The latter is essential for burning aneutronic fuels, which would ease engineering and environmental problems [2]. Many physics challenges remain for the FRC to be developed into a practical power plant: adequate energy confinement, stability against the internal tilt mode [3], and methods to sustain the plasma configuration and to heat the ions [4] to fusion-relevant temperatures [5]. The FRC is unique among toroidal magnetic confinement devices in that it is simply connected and has zero toroidal magnetic field, no internal conductor, and a line of zero magnetic field (within the plasma) encircling its major axis.

This paper examines ion heating by a new class of rotating magnetic fields, those of odd parity about the midplane [6]. Odd-parity modes may improve energy confinement by maintaining field closure.

Rotating magnetic fields (RMFs) have been used, particularly in rotamak devices [7,8], to make plasma, drive toroidal current, and obtain field reversal. Most studies of RMFs in rotamaks [9] considered only electron motion because the RMF frequency, ω_R, was chosen to be large compared to the ion-cyclotron frequency in the RMF, ${}_R\omega_{ci} \equiv q_i B_R/M_i c$, with q_i and M_i the charge and mass of the ion and B_R the RMF amplitude. The ion motion was assumed to be a mere quiver, not of any importance. However, to minimize circulating power, B_R in an FRC reactor must be much weaker than the main axial field, B_a. Then the condition $\omega_R \gg {}_R\omega_{ci}$ does not preclude $\omega_R \sim \omega_{ci} \equiv q_i B_a/M_i c$, the ion-cyclotron frequency in the main axial field. This broad resonance is shown here to be an effective ion-heating mechanism.

Previous studies of ion motion in RMFs have missed this effect because they were in different regimes of frequency, field strength, and duration. Ion motion in FRCs with even-parity, $\omega_R \gg \omega_{ci}$, RMFs has been analyzed for durations up to 250 gyroperiods [10,11]. These relatively short-time-scale studies showed no ion heating. In contrast, we have examined effects of odd-parity RMFs on ion orbits in an FRC for which $\omega_R \sim \omega_{ci}$ and find conditions, for both laboratory-scale experiments and reactors, under which ions are explosively heated to energies sufficiently high to be fusion relevant. For $B_R/B_a \sim 10^{-3}$, typically more than 1000 gyroperiods are necessary for appreciable heating. We note, in passing, that stability against the tilt mode is improved by energetic ions [12,13] and perhaps by the RMF itself [14].

The physical mechanism for this heating has limited similarities to ion-cyclotron-range-of-frequency (ICRF) heating [15,16]. The link is weak because the FRC's 3D geometry with steep gradients [17] does not provide a distinct resonance region. Also different from ICRF heating are the purely inductive nature of the FRC's electric field, the global departure from adiabaticity, and the relatively weak plasma response due to the assumed synchronous rotation of the electrons with the fully penetrated RMF.

RMF penetration is stated [9] to be controlled by the ratio of two dimensionless numbers, γ (the ratio of electron cyclotron frequency in the RMF field to the electron-ion collision frequency) and λ (the ratio of the separatrix radius to the classical skin depth). When $\gamma/\lambda > 1.2$, good penetration is predicted. For the specific FRC considered below, $\gamma/\lambda \sim 5$.

There is also a weak similarity to Fermi acceleration [18], (FA), in which a particle in a box gains energy by colliding with an oscillating wall. When an odd-parity RMF is applied to a "plasma-less" FRC, periodic axial and radial expansion and contraction of the closed field lines (flux surfaces) occur [6], similar to moving walls in FA. However, this picture is too simplistic. First, the "moving magnetic walls" of the FRC are soft compared with the standard FA hard-wall models; particles gain energy throughout the volume, not just at the boundaries. Second, particle acceleration is due to the time-varying **E** and **B**

 0031-9007/00/85(24)/5114(4)$15.00

fields and may be perpendicular or parallel to the moving magnetic walls. Finally, the FRC-RMF geometry is fully 3D, hence no KAM surfaces should exist and Arnold diffusion and Lévy trajectories are expected [19].

Our study is of single-particle trajectories in the fields of the FRC and RMF. This is appropriate if the collisionality is sufficiently low. A low-collisionality criterion is that the ratio of system size, r_s, to collision length, λ_c, be small, i.e., $r_s/\lambda_c < 0.1$. For Coulomb collisions, this corresponds to $E_m^2/n_i r_s > 10^{-11}$, where r_s (cm) is the separatrix radius of the FRC, E_m (eV) is the minimum ion energy, and n_i (cm^{-3}) is the plasma density. At $n_i = 10^{14}$ cm^{-3}, $E_m = 100$ eV for a 10-cm radius device. The explosive heating described here allows particles to make a quick transition from marginally collisional to fully collisionless.

The confining magnetic field of the FRC is described inside the separatrix as an elongated Hill vortex [17], $rA_\phi = \psi_0(r^2/r_s^2)(1 - r^2/r_s^2 - z^2/z_s^2)$ with A_ϕ the azimuthal vector potential, $\psi_0 = B_a r_s^2/2$, and B_a the field strength at the midpoint. The x points are at $\pm z_s$. To be fusion relevant, the final ion energy must exceed ~10 keV for D-T and ~40 keV for D-He_3 [20]. This imposes constraints on the size and field strength. For the sample calculations shown later, we fix $B_a = 20$ kG. At this field, deuterium ions have $\omega_{ci} \sim 10^8$ Hz and 3.6 MeV α particles (fusion-reaction products) have a 10-cm gyroradius. We assume the FRC to be elongated, $\kappa \equiv z_s/r_s = 5$, due to the favorable effect on tilt stability and, as shown below, to improve heating. We designate this as the reference FRC (RFRC). The vacuum field specified outside the separatrix [21] forms magnetic cusps near the x points, at elevations of $z \sim \pm 52$ cm. Low confining field strength near the x points and in the cusp region outside the separatrix creates potential loss channels for ions. The vector potentials for the odd-parity RMF are given by $(A_r, A_z, A_\phi)_{\mathrm{odd}} = (2B_R/k)[I_0(\xi)\cos kz \times \sin\psi, -I_1(\xi)\sin kz \sin\psi, I_0(\xi)\cos kz \cos\psi]$ where $\psi \equiv \phi - \omega_R t$, $\xi \equiv kr$, $k = l\pi/\kappa r_s$ is the wave number of the RMF, l is the axial mode number, and the I_m are modified Bessel functions. Near $z = 0$, the axial component A_z and the electric field due to its time derivative are small compared to the corresponding r and ϕ components.

Using a computer code RMF_1.13, we numerically integrate the six nonlinear differential equations comprising Hamilton's equations, $H = (1/2M_i)[(p_r - q_i A_r/c)^2 + (p_z - q_i A_z/c)^2 + (1/r^2)(p_\phi - q_i r A_\phi/c)^2]$: $\dot{r} = \partial H/\partial p_r$, $\dot{z} = \partial H/\partial p_z$, $\dot{\phi} = \partial H/\partial p_\phi$, $\dot{p}_r = -\partial H/\partial r$, $\dot{p}_z = -\partial H/\partial z$, and $\dot{p}_\phi = -\partial H/\partial \phi$, with an adaptive multistep method [22]. No electrostatic potential is included; such a potential has been predicted [23], but has not been verified. It will be the subject of a future study. Because H depends on ϕ and t only through ψ, the transformed Hamiltonian $K \equiv H - \omega p_\phi$ is conserved. K is used to monitor the accuracy of numerical integration; it is conserved to a relative tolerance $\leq 10^{-3}$ in all runs reported here, even while some of these runs required $\sim 10^8$ integrator steps.

In a typical code run, a 100-eV deuteron is initialized at a position inside the RFRC's separatrix. Other initial parameters are the angles of the particle's velocity, and the phase, frequency, and amplitude of the RMF. Deuterons with 100 eV perform cyclotron orbits, unless they are very close to the O-point null line, in which case they may perform null-line-crossing betatron orbits. In an FRC, ion-cyclotron orbits drift in one toroidal direction, antiparallel to the FRC current, while betatron orbits drift in the opposite direction. (An intermediate class of null-line-crossing orbits, termed figure-8 orbits [24], may drift in either direction.) The sign of ω_R is positive when the RMF rotates in the direction of the ion-cyclotron drift.

These types of orbit-following calculations are similar to those performed for ions and electrons in the magnetotail [25]. Complicated dynamics, such as Speiser orbits [26], have been observed, even though the calculations were only 2D and time-dependent fields, such as an RMF, were not included in the analyses.

The amplitude of the RMF-generated electric field in the RFRC, $\mathbf{E} = -(\partial \mathbf{A}/\partial t)/c$, is $E \sim \omega_R r_s B_R/c \sim 10$ V/cm for $B_R = 1$ G and $\omega_R = \omega_{ci}$. This field causes ion acceleration and deceleration, $dH/dt = q_i \mathbf{E} \cdot \mathbf{v}$, depending on the relative phase of the instantaneous electric field and the particle velocity. Acceleration predominates for low-energy particles.

For a typical code run, Fig. 1(a) shows deuteron energy H as a function of dimensionless scaled time $\tau = t/\tau_{ci}$, with τ_{ci} the ion-cyclotron period at the midpoint field, for $B_R = 20$ G, OMFAC $\equiv \omega_R/\omega_{ci} = +0.95$, and $k = \pi/50$, i.e., $l = 1$. The energy remains near 100 eV for $\tau < 800$. At $\tau \sim 910$, the energy begins an explosive growth from 400 eV to 6 keV, reached in $\Delta\tau \sim 50$. An enlarged view of this interval, Fig. 1(b), shows the main energy gains to occur in steps of half of an RMF period, displaying the absence of a sharp resonance. Energy-gaining steps are separated by several RMF periods. Returning to Fig. 1(a), the energy falls to less than 1 keV before growing to 17 keV at $\tau \sim 3.6 \times 10^3$, i.e., $t = 0.24$ ms. When this trajectory is followed further, to $\tau = 8 \times 10^4$, the maximum energy rises only slightly, to 19.2 keV. In this simulation there is no evidence for diffusion to higher energies. The average energy over this run is 6.6 keV.

Most of the energy is gained from the r and ϕ components of the RMF electric field, not from the weaker z component. As will be shown later, energy gain is strongly correlated with an RMF frequency in the ion-cyclotron frequency range, although the strong variation of the confining magnetic field strength precludes a sharp or continuous resonance. As a result, energy gain is primarily transverse to the confining magnetic field, contributing to high-energy particles being well confined and preferentially localized to the neighborhood of the midplane. Figure 1(c) shows

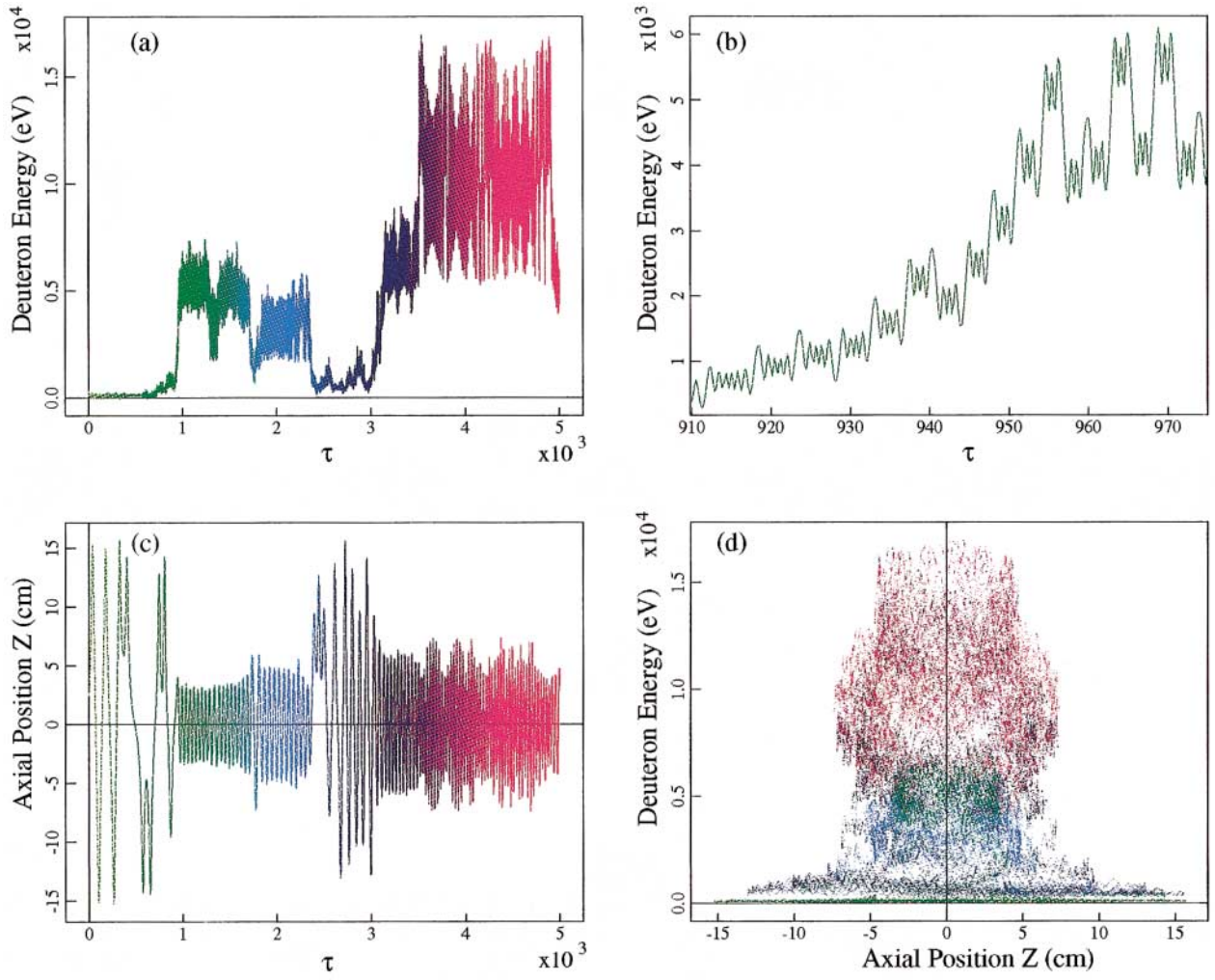

FIG. 1 (color). In this figure, color coding is used to distinguish successive time intervals. (a) Deuteron energy versus scaled dimensionless time $\tau = \omega_{ci}t/2\pi$. (b) Enlarged view of deuteron energy versus τ during a period of explosive growth. (c) Deuteron axial position z versus τ. (d) Deuteron energy versus axial position.

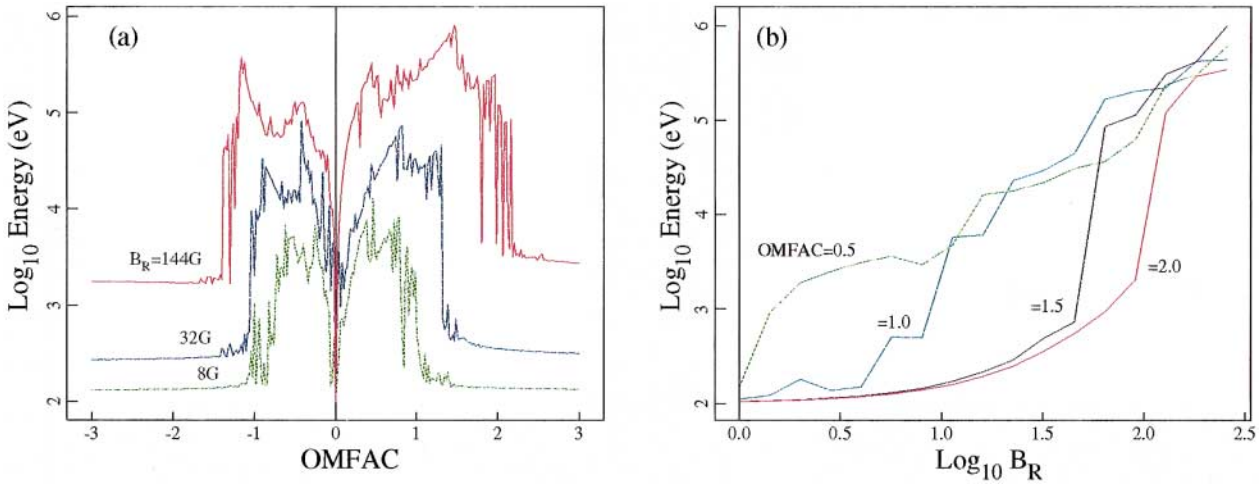

FIG. 2 (color). (a) Maximum energy attained by deuterons in the RFRC versus OMFAC $\equiv \omega_R/\omega_{ci}$ for $B_R = 8$, 32, and 144 G and $\tau = 10^4$. OMFAC was varied in steps of size 0.02. (b) Maximum energy attained by deuterons in the RFRC versus B_R for OMFAC = 0.5, 1.0, 1.5, and 2.0, and $\tau = 10^4$.

the z position of the same orbit as a function of scaled time τ. At early times, $\tau < 900$, when the deuteron has low energy, its orbit frequently stagnates near the z extrema of the initial flux surface, $z \sim \pm 13$ cm, due to Speiser collisions, i.e., nonconservation of magnetic moment, and mirror trapping. After the energy grows to 5 keV at $\tau \sim 1000$, the orbit is localized to $|z| < 3$ cm. The correlation between high energy and small $|z|$ is also seen in Fig. 1(d).

Figure 2 presents surveys of the dependences of the maximum deuteron energy on RMF frequency and amplitude. Figure 2(a) shows, for $B_R = 8$, 32, and 144 G, the maximum energy attained within $\tau = 10^4$. Figure 2(b) shows the variation of maximum energy with B_R for fixed OMFAC $= 0.5$, 1.0, 1.5, and 2.0. Important results are the following: (1) heating is greatest in the ion-cyclotron range of frequencies, $0.1 < |\text{OMFAC}| < 1$, with the upper limit increasing with B_R; (2) heating to fusion-relevant energies is independent of RMF rotation direction; (3) only a relatively small amplitude RMF, $\sim 0.1\%$ of the axial field, is required to heat to fusion-relevant energies; and (4) heating increases strongly above a threshold amplitude of B_R, which depends on OMFAC. Figure 2(a) is asymmetric about OMFAC $= 0$, with high attained energies extending to higher OMFAC values for positive OMFAC. This is qualitatively consistent with the Doppler-shifted RMF frequency seen by deuterons performing betatron orbits. The sharp boundary to the maximum energy attained at positive OMFAC may be useful for the selective heating of He_3 in D-He_3 mixtures.

For a heating duration of $\tau = 10^4$, the scaling of maximum energy attained is found to be approximately $E_{\max} \sim \omega_R^0 B_a^2 B_R^{1.5} \kappa^{1/2} r_s^2$ for parameters in the ranges $0.1 < |\text{OMFAC}| < 1$, $1 < \kappa < 10$, $1 < r_s < 40$ cm, $10^{-4} < B_R/B_a < 10^{-2}$, and $0.1 < B_a < 10$ T.

If an ion reaches the X-point region, it may be lost. For the RFRC, the loss rate, negligible at $B_R = 20$ G, increases markedly above $B_R = 50$ G. The self-consistent electrostatic potential and alternative magnetic boundary conditions may affect losses.

In summary, we have shown that small-amplitude odd-parity rotating magnetic fields can be used in modest-sized FRC devices to heat ions to fusion-relevant energies. The orbits of the high-energy ions preferentially localize near the midplane, which could have good implications for energy confinement, stability, and fusion reactivity. Moreover, the high-energy-ion orbits are of the betatron type, and may contribute to sustaining the FRC's current. The fully 3D model with strong field gradients should be of considerable interest in the general area of multidimensional chaos [27].

We thank J. R. Cary, J. P. Freidberg, P. Kevrekidis, M. A. Lieberman, and R. D. Milroy for useful discussions and E. E. Torbert for numerical calculations. This work was supported, in part, by the U.S. Department of Energy Contract No. DE-AC02-76-CHO-3073.

[1] For a review, see M. Tuszewski, Nucl. Fusion **28**, 2033 (1988).
[2] D. C. Barnes *et al.,* Fusion Technol. **30**, 116 (1996).
[3] M. N. Rosenbluth and M. N. Bussac, Nucl. Fusion **19**, 489 (1979).
[4] M. Lampe and W. Mannheimer, Naval Research Laboratory Report No. NRL/MR/6709-98-8305.
[5] N. Rostoker, M. Binderbauer, and H. Monkhorst, Science **278**, 1419 (1997).
[6] S. A. Cohen and R. D. Milroy, Phys. Plasmas **7**, 2539 (2000).
[7] H. A. Blevin and P. C. Thonemann, Nucl. Fusion Suppl. Pt. 1, 55 (1962).
[8] I. R. Jones, Phys. Plasmas **6**, 1950 (1999).
[9] For example, R. D. Milroy, Phys. Plasmas **6**, 2771 (1999).
[10] W. N. Hugrass and I. R. Jones, J. Plasma Phys. **29**, 155 (1983).
[11] W. N. Hugrass and M. Turley, J. Plasma Phys. **37**, 1 (1987).
[12] D. C. Barnes, J. L. Schwarzmeier, H. R. Lewis, and C. E. Seyler, Phys. Fluids **29**, 2616 (1986).
[13] L. C. Steinhauer and A. Ishida, Phys. Fluids B **2**, 2422 (1990).
[14] S. A. Cohen, Bull. Am. Phys. Soc. **44**, 586 (1999).
[15] For a summary, see T. H. Stix, *Waves in Plasmas* (American Institute of Physics, New York, 1992), Chaps. 11 and 13.
[16] A. Bécoulet, D. J. Gambier, and A. Samian, Phys. Fluids B **3**, 137 (1991).
[17] L. S. Solov'ev, in *Reviews of Plasma Physics 6,* edited by M. Leontovitch (Consultants Bureau, New York, 1976), p. 239.
[18] For a review, see A. J. Lichtenberg and M. A. Lieberman, *Regular and Stochastic Motion* (Springer-Verlag, New York, 1983).
[19] M. A. Lieberman and A. J. Lichtenberg, Phys. Rev. A **5**, 1852 (1972).
[20] J. M. Dawson, in *Fusion,* edited by E. Teller (Academic Press, New York, 1981), Vol. B, p. 492.
[21] L. E. Zakharov and V. D. Shafranov, in *Reviews of Plasma Physics 11,* edited by M. Leontovitch (Consultants Bureau, New York, 1986), p. 206.
[22] A. C. Hindmarsh, in *Scientific Computing,* edited by R. S. Stepleman *et al.* (North-Holland, Amsterdam, 1983), pp. 55–64.
[23] W. N. Hugrass, J. Plasma Phys. **28**, 369 (1982).
[24] J. M. Finn and R. N. Sudan, Nucl. Fusion **22**, 1443 (1982).
[25] For a review, see J. Chen, J. Geophys. Res. **97**, 15 011 (1992).
[26] T. W. Speiser, J. Geophys. Res. **70**, 4219 (1965).
[27] G. M. Zaslavskii *et al.,* Sov. Phys. JETP **69**, 885 (1989).